



HYPERBOLICITY OF AN APROXIMATED FORM OF THE DRIFT FLUX MODEL APPLIED TO THE VERTICAL ASCENDANT GAS-LIQUID FLOW

Christiano Garcia da Silva Santim

Universidade Estadual de Campinas, CEP: 13083-860
chriss@fem.unicamp.br

Luiz Eduardo Melo Lima

Universidade Tecnológica Federal do Paraná, CEP: 84016-210
lelima@utfpr.edu.br

Eugênio Spanó Rosa

Universidade Estadual de Campinas, CEP: 13083-860
erosa@fem.unicamp.br

Abstract. *The motivation of this work is the development of a Riemann solver to the transient isothermal drift flux model, a set of two mass equations and one momentum equation which describes the transient behavior of a gas-liquid mixture in a pipe. The set of equations constitutes a non-linear hyperbolic system of conservation laws in one space dimension. The hyperbolicity is one of the main features of this system and rules the nature of the numerical methods employed to solve the system. The system is hyperbolic as long as the three eigenvalues of the Jacobian matrix, \mathbf{A} , are real and distinct. The present article objective is the development of approximated forms of \mathbf{A} to express the eigenvalues by means of analytical expressions in order to reduce the computational cost of the Riemann solver. The simplification hypothesis considers the squared of sound velocities ratio between the gas to the liquid phases much smaller than one. The approximated form of \mathbf{A} and the hiperbolicity analysis is performed for a range of gas and liquid superficial velocities spanning from 0.1 to 28 m/s and for operational pressures of 1, 10 and 100 bar. Furthermore the accuracy of the approximated eigenvalues expressions are compared against the exact value resulting in an accuracy better than 3% for applications where the void fraction spans from 0.15 to 0.98.*

Keywords: *Drift flux model, Riemann solver, transient, gas-liquid flow*

1. INTRODUCTION

The motivation of this work is the development of a Riemann solver to the transient isothermal drift flux model. The choice for a Riemann solver instead of numerical schemes based on finite differences or finite volumes is fact that the former embodies on the numerical routines physical aspects of the phenomena. The wave decomposition discloses if the faster or the slower wave families are dominant on the flow field and the characteristic velocities reveals the flow characteristic times. Furthermore, the numerical method only works if the system is hyperbolic, i.e., if the system has real and distinct eigenvalues. The loss of system's hiperbolicity frequently is signal that some of the closure equations are inappropriate to the present flow regime.

The transient flow of a gas-liquid mixture inside a pipe is expected to behavior physically as a wave which has a finite propagation velocity and the flow along the pipe exhibits zones of influence and zones of dependence as it advances in time. The three transient equations representing the drift flux model constitutes a non-linear hyperbolic system of conservation laws in one space dimension which mathematically represents the expected wave behavior of the gas-liquid mixture. The hyperbolicity is the main feature of this system and rules the nature of the numerical methods employed to solve the system. As a first step toward development of a Riemann solver this work presents the development of a hiperbolicity analysis of a simplified form of drift flux set of equations.

In previous work Theron (1989) and Gavage (1991) developed simplified forms of the drift flux model to the Jacobian matrix \mathbf{A} and to express the eigenvalues through simple analytical expressions. More recently Fjelde and Karlsen (2000) propose the use of numerical techniques to evaluate the exact form of the Jacobian matrix \mathbf{A} . While Fjelde and Karlsen (2000) approach is exact it has a high computational cost to use in Riemann solvers. On the other hand the simplifications used by Theron (1989) and Gavage (1991) over simplify the non-linear system constraining its application range on gas-liquid flows. Flatten and Munkejord (2006) constructed a Roe-type numerical scheme for approximating the solutions of a drift flux two phase flow model. The authors derived an analytical expression for the flux Jacobian of the model. A method for obtaining a fully-analytical Roe matrix for the special case of the Zuber-Findlay closure law was presented.

Based on the exact representation of the drift flux system an analytical expression to the Jacobian matrix \mathbf{A} is developed by the recursive use of implicit derivatives. The elements of matrix \mathbf{A} are further simplified considering the simplifying hypothesis where the sound velocity ratio of the gas to the liquid phases is $(c_g/c_l)^2 \ll 1$. To test the hyperbolicity of the simplified system the eigenvalues are evaluated analytically and compared against the exact values.

2. MATHEMATICAL FORMULATION

The one dimensional, transient, isothermal and no interphase mass transfer form of the drift flux model is shown in Eqs. (1) thru (3). Equations (1) and (2) represent the mass conservation on the liquid and gas phases and the mixture momentum equation is shown in Eq. (3).

$$\frac{\partial}{\partial t}[(1-\alpha)\rho_l] + \frac{\partial}{\partial x}[(1-\alpha)\rho_l v_l] = 0, \quad (1)$$

$$\frac{\partial}{\partial t}(\alpha\rho_g) + \frac{\partial}{\partial x}(\alpha\rho_g v_g) = 0, \quad (2)$$

$$\frac{\partial}{\partial t}[(1-\alpha)\rho_l v_l + \alpha\rho_g v_g] + \frac{\partial}{\partial x}[(1-\alpha)\rho_l v_l^2 + \alpha\rho_g v_g^2 + p] = s_m, \quad (3)$$

where p is the pressure, α is the gas void fraction, the subscripts l and g identify the liquid and gas phases and are associated to the fluids density and velocity, ρ and v respectively. The last term on Eq. (3), s_m , is a source term representing the wall friction force and possible volumetric forces, e.g., gravity. Since the term s_m has no space or time derivative associated with it the hyperbolicity analysis is performed only with homogenous part of the system and there is no need to define s_m for the moment.

The thermodynamic state equations for the liquid and gas densities are expressed in terms of the sound velocities

$$\rho_l = \rho_{l,0} + \frac{p - p_{l,0}}{c_l^2} \quad \text{and} \quad \rho_g = \frac{p}{c_g^2} \quad (4)$$

where the velocity of the sound to the liquid phase is represented by c_l and $\rho_{l,0}$ and $p_{l,0}$ are given constants. Due to the heat capacities difference between the gas and liquid phases the sound velocity for the gas phase is evaluated considering an isothermal process, $c_g = \sqrt{RT_0}$ where T_0 is the reference temperature and R is the gas constant. Surface tension effects are not considered therefore it is expect from Eq. (4) that $(\rho_l - \rho_{l,0}) \cdot c_l^2 + p_{l,0} = \rho_g \cdot c_g^2$.

The system of equations given by Eqs. (1) thru (3) can be expressed in the conservative form in terms of the vectors of the variables and of the fluxes, \mathbf{U} and \mathbf{F} respectively

$$\frac{\partial \mathbf{U}}{\partial t} + \frac{\partial \mathbf{F}}{\partial x} = 0 \quad \text{where} \quad \mathbf{U} = \begin{pmatrix} u_1 \\ u_2 \\ u_3 \end{pmatrix} \equiv \begin{pmatrix} (1-\alpha)\rho_l \\ \alpha\rho_g \\ (1-\alpha)\rho_l v_l + \alpha\rho_g v_g \end{pmatrix} \quad \text{and} \quad \mathbf{F} = \begin{pmatrix} f_1 \\ f_2 \\ f_3 \end{pmatrix} \equiv \begin{pmatrix} (1-\alpha)\rho_l v_l \\ \alpha\rho_g v_g \\ (1-\alpha)\rho_l v_l^2 + \alpha\rho_g v_g^2 + p \end{pmatrix} \quad (5)$$

The system has three equations and four unknowns. To provide the system closure it is used the kinematic relation proposed by Zuber and Findlay (1965).

$$v_g = C_0 v_m + v_d, \quad (6)$$

where v_m is the mixture velocity and v_d is the drift velocity as defined in Eq. (7).

$$v_m = (1-\alpha)v_l + \alpha v_g \quad \text{and} \quad v_d = C_\infty \sqrt{\left(1 - \frac{\rho_g}{\rho_l}\right) g D} \quad (7)$$

The parameters C_0 and C_∞ employed in Eqs.(6) and (7) are defined accordingly to the fluids transport properties and to the flow pattern regime. Table 2 exhibits the values for C_0 and C_∞ as a function of the flow pattern regime.

2.1 The Jacobian matrix and the eigenvalues

The Jacobian matrix \mathbf{A} arises when Eq.(5) is expressed by its quasi-linear form

$$\frac{\partial \mathbf{U}}{\partial t} + \mathbf{A} \frac{\partial \mathbf{U}}{\partial x} = 0, \quad \text{with} \quad \mathbf{A} = \frac{d\mathbf{F}}{d\mathbf{U}} = \begin{bmatrix} \frac{df_1}{du_1} & \frac{df_1}{du_2} & \frac{df_1}{du_3} \\ \frac{df_2}{du_1} & \frac{df_2}{du_2} & \frac{df_2}{du_3} \\ \frac{df_3}{du_1} & \frac{df_3}{du_2} & \frac{df_3}{du_3} \end{bmatrix} \quad (8)$$

The difficult task to get the elements of the Jacobian matrix is to evaluate the derivatives of the components of the vector flux to the components of the vector of variables as indicated in Eq.(8). The employed technique resembles the thermodynamics derivatives. The procedure is shown in the form of an example to evaluate the element \mathbf{A}_{1x1} .

$$\mathbf{A}_{1x1} = \left. \frac{df_1}{du_1} \right|_{u_2, u_3} = -\rho_l v_l \left. \frac{d\alpha}{du_1} \right|_{u_2, u_3} + (1-\alpha) v_l \left. \frac{d\rho_l}{du_1} \right|_{u_2, u_3} + (1-\alpha) \rho_l \left. \frac{dv_l}{du_1} \right|_{u_2, u_3} \quad (9)$$

The evaluation of the 1st and 3rd terms of the RHS of Eq. (9) is straightforward but the evaluation of the 2nd term is not trivial. Therefore this example focus on the evaluation of $d\rho_l/du_1|_{u_2, u_3}$. Expressing ρ_l by the state equation defined in Eq. (4) then

$$\left. \frac{d\rho_l}{du_1} \right|_{u_2, u_3} = \left. \frac{1}{c_l^2} \frac{dp}{du_1} \right|_{u_2, u_3} \quad (10)$$

Considering that $u_l = u_l(\alpha, \rho_l)$ then

$$\left. \frac{du_l}{dp} \right|_{\alpha} = \left. \frac{du_l}{d\rho_l} \frac{d\rho_l}{dp} \right|_{\alpha} + \left. \frac{du_l}{d\alpha} \frac{d\alpha}{dp} \right|_{\rho_l} \quad (11)$$

Using again the state equation for the liquid phase to express

$$\left. \frac{d\rho_l}{dp} \right|_{\alpha} = \frac{1}{c_l^2}, \quad (12)$$

and since u_2 is held constant in Eq.(10) and $d\rho_g = dp/c_g^2$, it is possible to define

$$\left. \frac{dp}{d\alpha} \right|_{u_2} = -\frac{\rho_g c_g^2}{\alpha} \quad (13)$$

Substituting Eqs. (12) and (13) into Eq. (11) one gets

$$\left. \frac{du_l}{dp} \right|_{\alpha} = \frac{(1-\alpha)}{c_l^2} + \frac{\rho_l}{\rho_g} \frac{\alpha}{c_g^2} \quad (14)$$

Applying the law of reciprocal of the derivatives in Eq. (14) and replacing the result in Eq. (10) one gets

$$\left. \frac{d\rho_l}{du_1} \right|_{u_2, u_3} = -\frac{c_g^2}{c_l^2} \frac{\left(\frac{\rho_g}{\rho_l} \right)}{\left(\frac{\rho_g}{\rho_l} \right) \cdot \left(\frac{c_g^2}{c_l^2} \right) (1-\alpha) + \alpha} \quad (15)$$

The analytical expressions defining the next elements of \mathbf{A} are evaluated following similar procedure. The nine elements of \mathbf{A} are rather lengthy analytical expressions. This work proposes a simplification hypothesis on the elements of \mathbf{A} neglecting terms where

$$\left(c_g/c_l \right)^2 \ll 1 \quad (16)$$

C.G.S., Santim, L.E.M., Lima and E.S., Rosa

Aproximated Eigenvalues and Hyperbolicity of the Drif Flux Model Applied to the Vertical Gas-Liquid Flow

Applying the hypothesis defined in Eq. (16) on the exact form of \mathbf{A} one gets the approximated form of the Jacobian matrix where the elements of the 1st, 2nd and 3rd lines are displayed in Table 1.

Table 1. Aproximated form of the Jacobian matrix when $(c_g/c_l)^2 \ll 1$.

$\mathbf{A}_{1x1} = v_g \frac{C_0 \alpha \left(\frac{\rho_g}{\rho_l} \right)}{1 - C_0 \alpha \left(1 - \frac{\rho_g}{\rho_l} \right)}$	$\mathbf{A}_{1x2} = -v_g \frac{(1 - C_0 \alpha)}{1 - C_0 \alpha \left(1 - \frac{\rho_g}{\rho_l} \right)}$	$\mathbf{A}_{1x3} = \frac{1 - C_0 \alpha}{1 - C_0 \alpha \left(1 - \frac{\rho_g}{\rho_l} \right)}$
$\mathbf{A}_{2x1} = -v_g \frac{C_0 \alpha \left(\frac{\rho_g}{\rho_l} \right)}{1 - C_0 \alpha \left(1 - \frac{\rho_g}{\rho_l} \right)}$	$\mathbf{A}_{2x2} = v_g \frac{(1 - C_0 \alpha)}{1 - C_0 \alpha \left(1 - \frac{\rho_g}{\rho_l} \right)}$	$\mathbf{A}_{2x3} = \frac{C_0 \alpha \left(\frac{\rho_g}{\rho_l} \right)}{1 - C_0 \alpha \left(1 - \frac{\rho_g}{\rho_l} \right)}$
$\mathbf{A}_{3x1} = \frac{\rho_l \left(c_g^2 \left(\frac{\rho_g}{\rho_l} \right) - v_l^2 \alpha \right) + C_0 \alpha \left(c_g^2 \rho_g \left(\frac{\rho_g}{\rho_l} - 1 \right) + \alpha \left(-2v_g^2 \rho_g + 2v_g v_l \rho_g + v_l^2 \rho_l \left(1 - \frac{\rho_g}{\rho_l} \right) \right) \right)}{\alpha \rho_l \left(1 - C_0 \alpha \left(1 - \frac{\rho_g}{\rho_l} \right) \right)}$		
$\mathbf{A}_{3x2} = \frac{\left(c_g^2 + v_g \alpha (v_g - 2v_l) \right) - C_0 \alpha \left(c_g^2 \left(1 - \frac{\rho_g}{\rho_l} \right) + v_g \alpha \left(-2v_l + v_g \left(\frac{\rho_g}{\rho_l} + 1 \right) \right) \right)}{\alpha \left(1 - C_0 \alpha \left(1 - \frac{\rho_g}{\rho_l} \right) \right)}$		
$\mathbf{A}_{3x3} = \frac{2 \left(v_l + C_0 \alpha \left(v_g \left(\frac{\rho_g}{\rho_l} \right) - v_l \right) \right)}{1 - C_0 \alpha \left(1 - \frac{\rho_g}{\rho_l} \right)}$		

The advantages of expressing \mathbf{A} by a simpler analytical form lays on simpler eigenvalues expressions which will aid the development of a linearized solver for this non-linear system. The eigenvalues expressions for the simplified form of \mathbf{A} are determined employing the symbolic processing embodied on Mathematica software. The eigenvalue expressions are

$$\lambda_1^A = v_l \left[\frac{\frac{\alpha C_0}{(1 - C_0 \alpha)} \left(\frac{\rho_g}{\rho_l} \right) \left(\frac{v_g}{v_l} \right) + 1}{\frac{\alpha C_0}{(1 - C_0 \alpha)} \left(\frac{\rho_g}{\rho_l} \right) + 1} \right] + c; \quad \lambda_2^A = v_l \left[\frac{\frac{\alpha C_0}{(1 - C_0 \alpha)} \left(\frac{\rho_g}{\rho_l} \right) \left(\frac{v_g}{v_l} \right) + 1}{\frac{\alpha C_0}{(1 - C_0 \alpha)} \left(\frac{\rho_g}{\rho_l} \right) + 1} \right] - c; \quad \lambda_3^A = v_g, \quad (17)$$

where c , represents the expression

$$c = \frac{\sqrt{\rho_g c_g^2 \left(1 - C_0 \alpha + C_0 \alpha^2 \frac{(v_g - v_l)^2}{c_g^2} (C_0 \alpha - 1) + C_0 \alpha \frac{\rho_g}{\rho_l} \right)}}{\sqrt{\alpha \rho_l \left(1 - C_0 \alpha + C_0 \alpha \frac{\rho_g}{\rho_l} \right)}} \quad (18)$$

The eigenvalues expressions resultants from the approximation $(c_g/c_l)^2 \ll 1$ on \mathbf{A} matches the eigenvalues proposed by Gavage (1991) in the limits where $(\rho_g/\rho_l) \ll 1$ and $(v_g - v_l)^2/c_g^2 \ll 1$ and by replacing $\rho_g c_g^2 = p$ as shown in Eq. (19)

$$\lambda_1^B = v_l + \sqrt{\frac{P}{\alpha \rho_l (1 - C_0 \alpha)}}; \quad \lambda_2^B = v_l - \sqrt{\frac{P}{\alpha \rho_l (1 - C_0 \alpha)}}; \quad \lambda_3^B = v_g \quad (19)$$

The match reveals physical consistency of the developed approach to a simpler formulation. While present work neglects terms with $(c_g/c_l)^2$ it is implied that the approach used by Gavage (1991) is even more constrained by neglecting terms of (ρ_g/ρ_l) and $(v_g - v_l)^2/c_g^2$ which for hypothesis have to be much smaller than one.

The accuracy of the simplified form of **A** shown in Table 1 is accessed by comparing the associated eigenvalues against the exact eigenvalues in section 3.

3. ANALYSIS AND RESULTS

The approximated Jacobian matrix hyperbolicity is accessed through an inspection on the eigenvalues expressions defined on Eqs.(17) and (18). If the eigenvalues are real and distinct the system of equations is hyperbolic (Whitham, 1974). The first and the second eigenvalues shown in Eq. (17) are linked to the gas compressibility and are generically represented by an expression of the form: $\lambda = u \pm c$ where u and c have velocity dimensions. Eventual shocks and rarefaction waves are associated with these eigenvalue families. The third eigenvalue shown in Eq. (17) is coincident to the gas phase velocity. There is no shock associated to this eigenvalue family, the pressure and velocity are continuous and it must represent a contact discontinuity in void fraction. The system hyperbolicity is assured as long the argument of the numerator of Eq. (18) is always greater than zero or simply

$$\frac{1}{C_0 \alpha^2} \left[1 + \frac{\rho_g/\rho_l}{1/(C_0 \alpha) - 1} \right] > \left(\frac{v_g - v_l}{c_g} \right)^2 > 0 \quad (20)$$

Equation (20) shows that the left term being bigger than the right term is not a sufficient condition. Since the term $(v_g - v_l)/c_g$ is squared it requires that the LHS be greater than zero or simply:

$$C_0 \alpha < 1 \quad (21)$$

The right side of Eq. (20) resembles a Mach number of a velocity difference. Considering transient flow phenomena related to gas-oil production lines in the petroleum industry, a conservative estimate would be $0.1 \leq [(v_g - v_l)/c_g]^2 \leq 0$. The left side of Eq. (20) is harder to estimate because it depends on the gas to liquid density ratio as well as on the C_0 and α values which in turn depends on the flow pattern regime. The analysis of the inequality has to be performed based on the procedures developed on the next section.

3.1 Numerical evaluation of the eigenvalues

In an attempt to amend the hyperbolicity test and at the same time to test the accuracy of the approximation done on the Jacobian matrix a series of numerical evaluations of eigenvalues using the parameters C_0 and C_∞ evaluated accordingly to the flow pattern regime.

The test scenario is an upward transient flow in a pipe with 0.025 m in diameter of an air-water mixture at ambient temperature and pressures of 1 bar, 10 bar and 100 bar. The pressure range was defined to match those found in oil production fields. The c_g is constant and equal to 292 m/s while c_l is assumed to be 1000 m/s. The water and air superficial velocities, J_l and J_g spanned from 0.1 to 5.2 m/s and from 0.1 to 28.1 m/s respectively. The phases superficial velocities are linked to the phases velocities through the void fraction proportionality

$$J_l = v_l (1 - \alpha) \quad \text{and} \quad J_g = v_g \alpha, \quad (22)$$

where the void fraction is estimated using Eq. (23).

$$\alpha = J_g / [C_0 (J_g + J_l) + v_d] \quad (23)$$

C.G.S., Santim, L.E.M., Lima and E.S., Rosa

Aproximated Eigenvalues and Hyperbolicity of the Drif Flux Model Applied to the Vertical Gas-Liquid Flow

To define a numerical value to the eigenvalues it is still necessary to define C_0 and C_∞ which are defined in Table 2 but flow pattern dependent.

Table 2. Definitions for the parameters C_0 and C_∞ .

Flow Pattern	C_0	C_∞
Uniform and distorted bubbles	$1 + 0.2\sqrt{\rho_g / \rho_l}$	$\sqrt{2}R_S^n Eo^{-0.25}$
Slug	1.2	$\frac{0.345}{(1 + 3805Eo^{-3.06})^{0.58}}$
Annular	$1 + \frac{R_F \left\{ 1 + \left[(3\pi DR_F / S_F - 4\delta) / (6C_{f,F}) \right]^{0.5} / Fr \right\}}{(1 - R_F) + \left[(C_{f,I} / C_{f,F}) (\rho_g / \rho_l) (S_I / S_F) / (1 - R_F) \right]^{0.5}}$	0
$Eo = \left[(\rho_l - \rho_g) g D^2 \right] / \sigma$ and $Fr = (J_l + J_g) / \sqrt{(\rho_l - \rho_g) g D / \rho_l}$		

The new variables displayed on Table 2 are defined as follow. The R_F and R_S are the liquid holdups for the liquid film and liquid piston when slug occurs; $C_{f,F}$ and $C_{f,I}$ are the Fanning friction factors to the liquid film and at the gas-liquid interface; S_F and S_I represent the perimeters of wetted by the film and of the interface; δ is the liquid film height and n applies for bubbly flow only and its value is 0 or 1.75 the bubbles are uniform or distorted. The values or expressions to the parameters C_0 and C_∞ for the bubbly, slug and annular flow patterns come from Hibiki and Ishii (2003), Bendkisen (1984) and Ishii *et al.* (1976). The churn flow is better characterized as a transition flow pattern between slug and annular flow. The values for C_0 and C_∞ are not well defined to this regime because being a transitional regime it is fuzzy. This work adopted for churn flow the same relations applied in slug. The shift on the C_0 and C_∞ parameters is performed accordingly to the flow pattern predicted by the Taitel *et al.* (1980) flow map for ascendant vertical flows as the J_l and J_g velocities changed along the test grid.

For referencing purposes Figure 1 displays the flow maps for pressures of 1 bar, 10 bar and 100 bar. The square lines represent the boundaries of the superficial velocities defined by the test grid. The open circles are sample points within the test grid used to display the evaluated void fraction. The void fraction values superposed into the flow map disclose a flow pattern dependency on the void fraction value. As J_g increases, α increases and the flow pattern changes are toward the annular flow. This dependence will be explored on the next section to display the eigenvalues map. The effect of the pressure change on the flow map is also noticeable. As the pressure increases the transition to the annular flow is moved to left; at 100 bar the churn flow no longer exists accordingly to this model.

3.2 Eigenvalues comparison

To access the accuracy of the approximated Jacobian matrix this matrix's eigenvalues, see Eqs.(17) and (18), are compared against the eigenvalues from the exact Jacobian matrix. Figure 2 shows, for reference purposes, the eigenvalues from the exact Jacobian matrix for pressures of 1 bar, 10 bar and 100 bar. For the range of pressures and phases velocities evaluated all the eigenvalues are real and distinct. The families λ_1 and λ_2 are presented in Figure 2a and 2b respectively. These eigenvalues families are linked to the gas compressibility and are generically represented by an expression of the form: $\lambda = u \pm c$. For being the sum or the difference of a reference velocity their behavior is analyzed together. The pressure has a strong effect on the eigenvalues. As the pressure increases the eigenvalues' absolute values increase for a given void fraction. At the extremes, $\alpha \rightarrow 0$ or $\alpha \rightarrow 1$ the mixture approaches the single phase flow of water or air, therefore the eigenvalues exhibits a tendency to approach this asymptotic values. The exact Jacobian matrix eigenvalues are lengthy expressions which make difficult a physical analysis to explain better the dependence on α and p . This will be postponed to the analysis of the eigenvalues expressions for the approximated Jacobian matrix. At last, the third eigenvalue is simply the air velocity, v_g . The representation of v_g against α result in decreasing curves because $v_g = J_g / \alpha$.

22nd International Congress of Mechanical Engineering (COBEM 2013)
 November 3-7, 2013, Ribeirão Preto, SP, Brazil

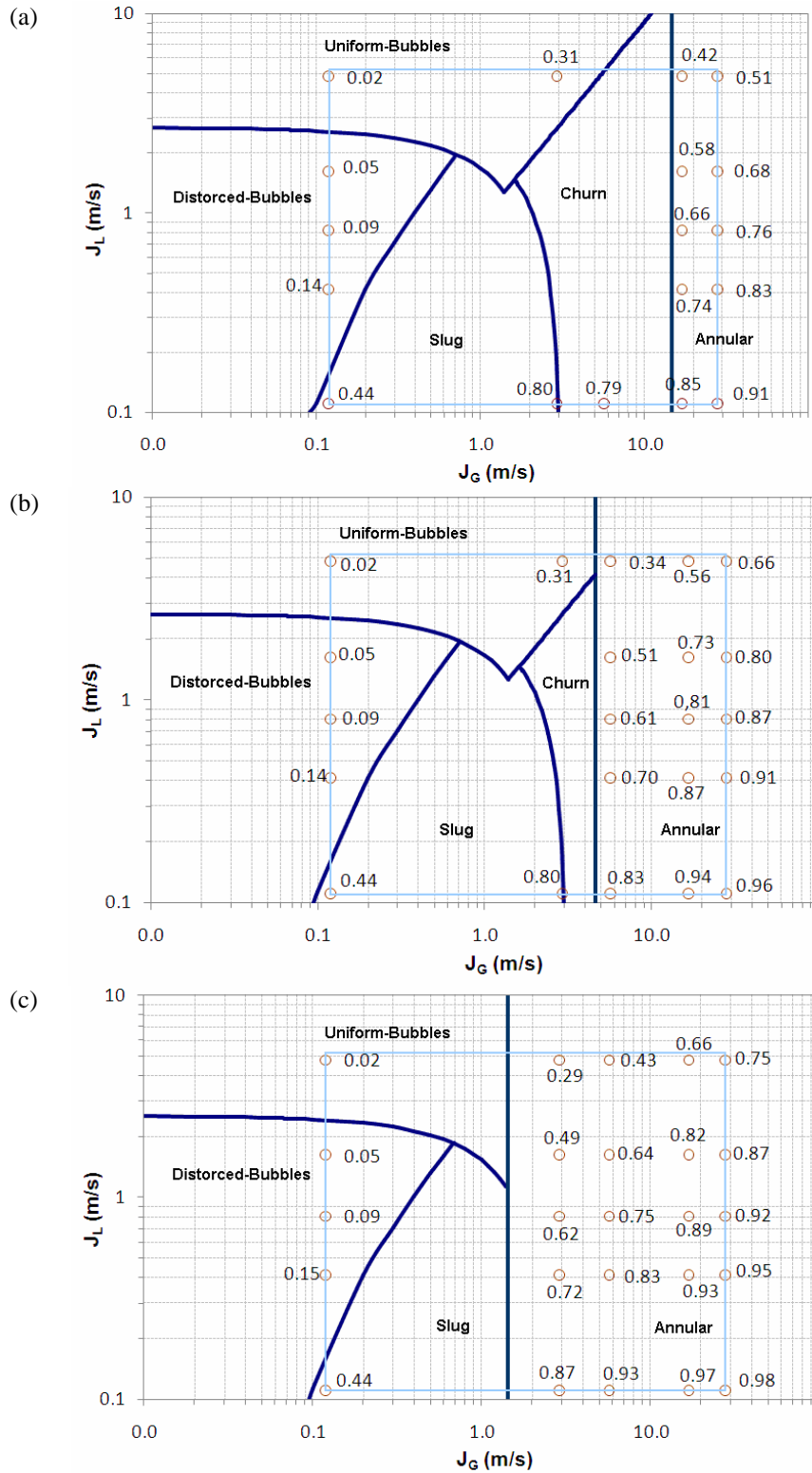


Figure 1. Flow map for (a) $p = 1$ bar; (b) $p = 10$ bar; (c) $p = 100$ bar.

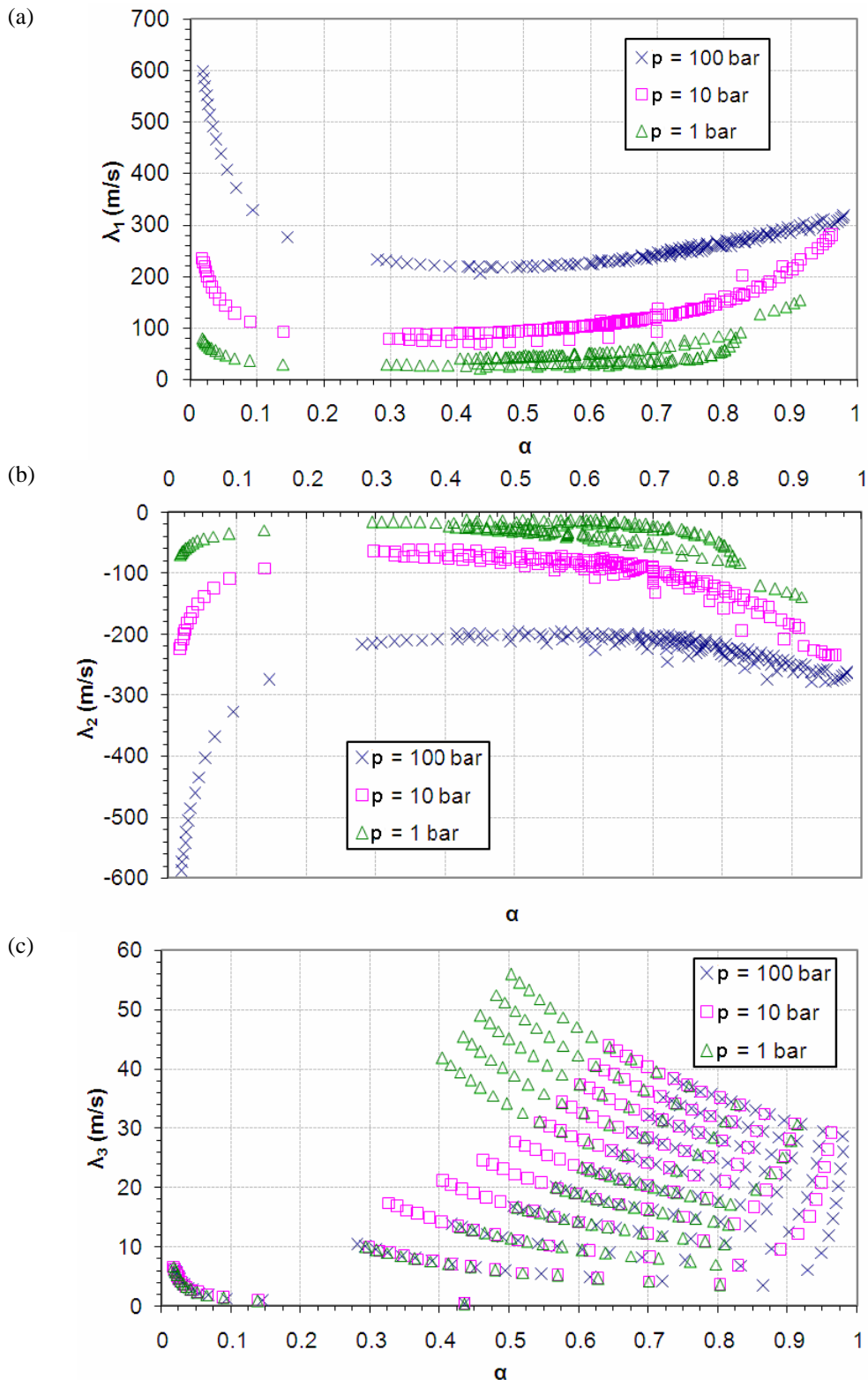


Figure 2. Eigenvalues families for the exact Jacobian matrix for pressures of 1 bar, 10 bar and 100 bar; λ_1 , λ_2 , and λ_3 in (a), (b) and (c) respectively.

Within the proposed test grid the eigenvalues resultant from the approximated Jacobian matrix, see Eqs. (17) and (18), and those proposed by Gavage (1991), see Eq. (19), are all real and distinct therefore the system is hiperbolic. The following test access the accuracy of the approximated Jacobian matrix by comparing the eigenvalues against the exact values show in Figure 2 in terms of the relative error given by

$$\text{Error (\%)} = \frac{|\lambda_{\text{simplified}} - \lambda_{\text{exact}}|}{\lambda_{\text{simplified}}} \times 100 \quad (24)$$

Figure 3a shows the relative error for λ_1^A eigenvalue family as a function of the void fraction for pressures of 1 bar, 10 bar and 100 bar. The relative error of the λ_1^A increases as the pressure increase or the void fraction decreases. Nonetheless for $\alpha > 0.3$ the relative error for all tested pressures is less than 1 % of the exact eigenvalue. For $\alpha < 0.3$ the relative error grows as the void fraction approaches zero and is sensitive to the operational pressure. For $\alpha = 0.01$ the relative errors were of 0.25 %, 2.5 % and 25 % for pressures of 1 bar, 10 bar and 100 bar respectively.

Figure 3b exhibits the Gavage (1991) approximated eigenvalue, λ_1^B . It is observed that the eigenvalues are also sensitive to the operational pressure but, distinctly from previous case, the behavior of relative error is described as a concave curve with a local minimum nearly at $\alpha = 0.25$. For $\alpha < 0.3$ the relative error behavior is coincident with the previous case but, for $\alpha > 0.3$ the relative error behavior diverge. For α ranging from 0.91 to 0.98 the relative errors are as high as 10 %, 100 % and 400 % for pressures of 1 bar, 10 bar and 100 bar respectively.

Figure 4a and 4b shows the relative error for λ_2^A and λ_2^B eigenvalues family as a function of the void fraction for pressures of 1 bar, 10 bar and 100 bar. The figure is shown just for completeness of the eigenvalues information but the relative error bounds and behavior are have the same description given form λ_1^A and λ_1^B families.

No comparison is made for λ_3 family because it is coincident with the exact value.

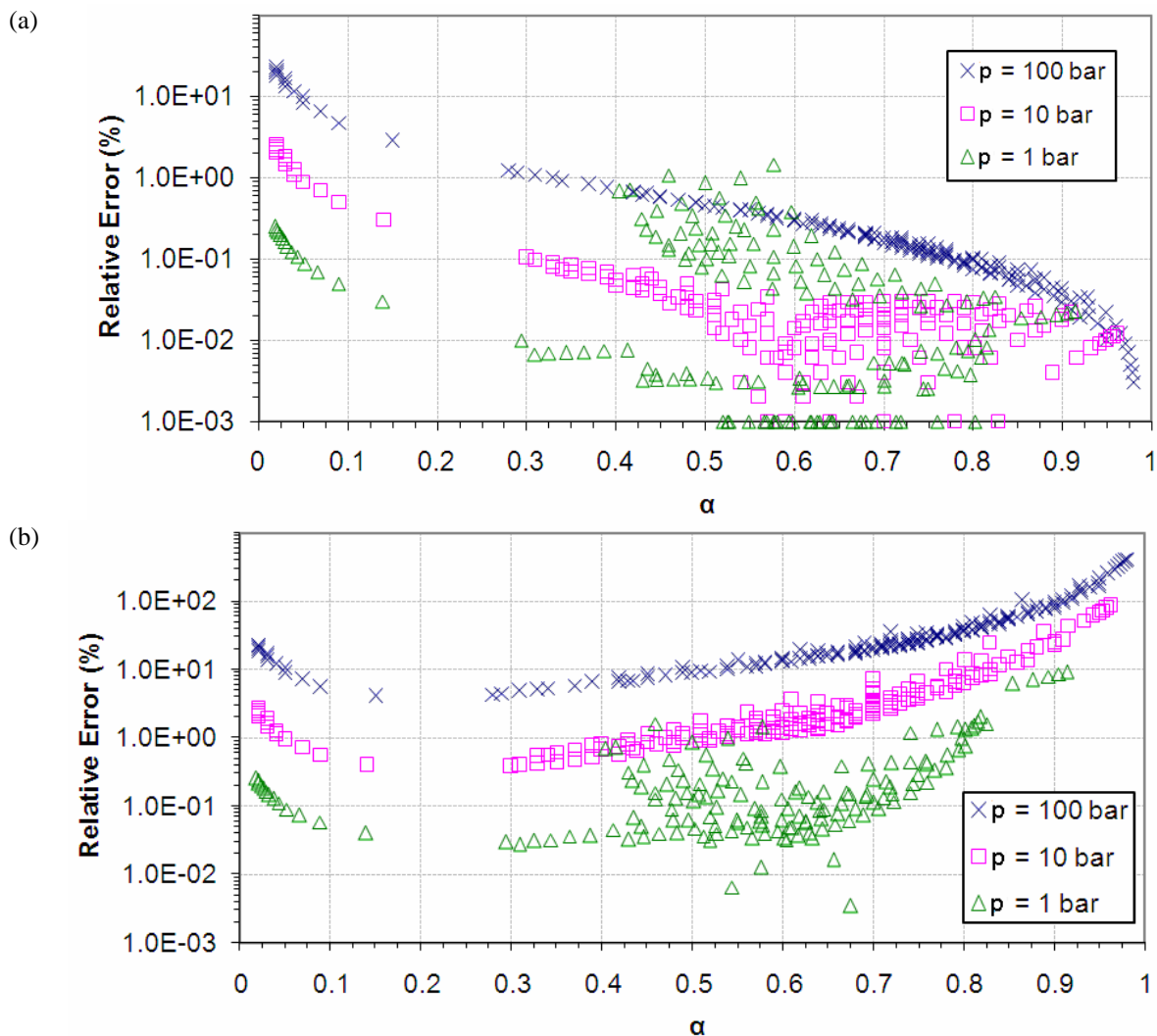


Figure 3. Relative error of λ_1^A (a) and λ_1^B (b) in terms of void fraction for different pressures.

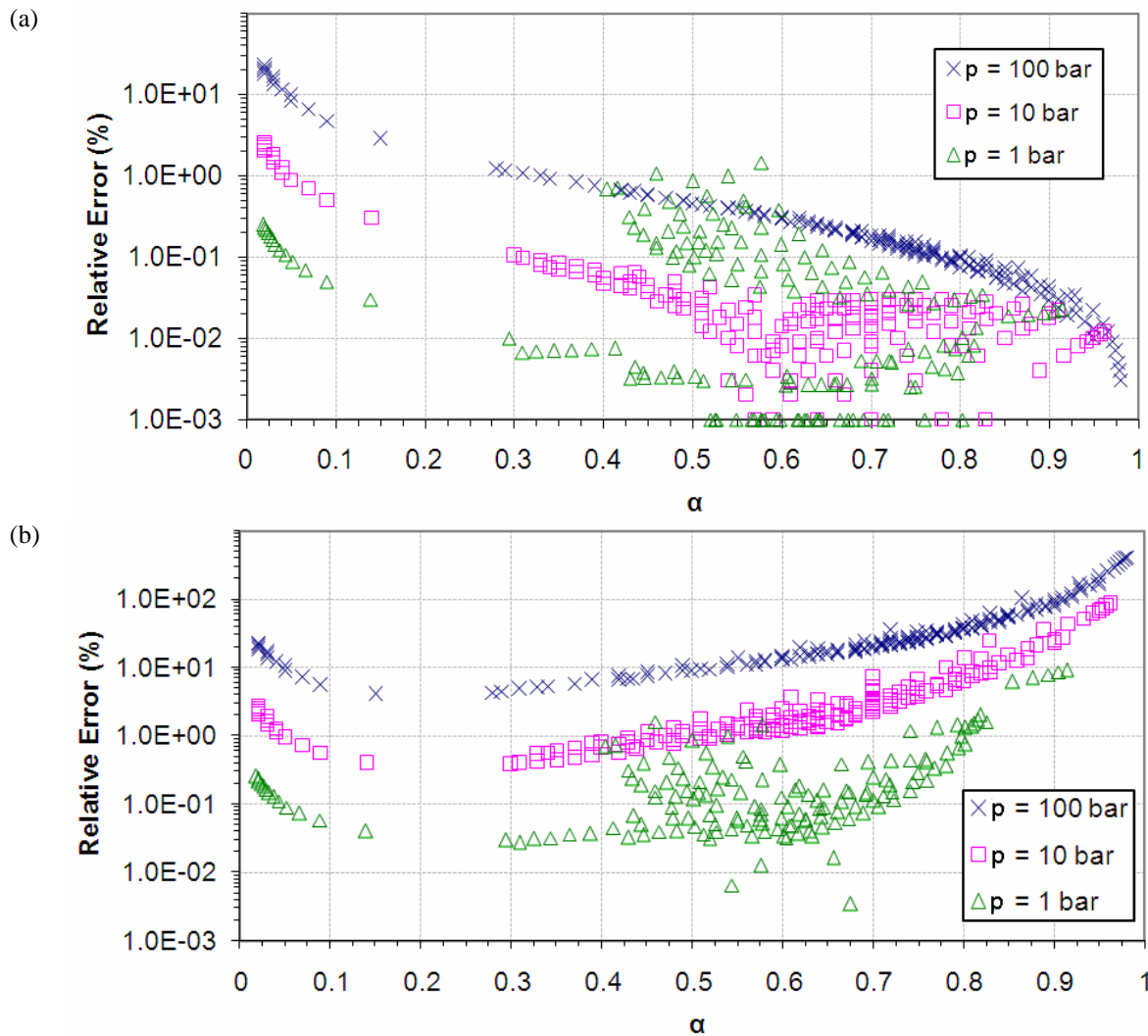


Figure 4. Relative error of λ_2^A (a) and λ_2^B (b) in terms of void fraction for different pressures.

The behavior of the exact eigenvalues shown in Figure 2 and the relative error behavior shown in Figures 3 and 4 for the $\lambda_{1,2}$ eigenvalues families can be interpreted rewritten Eq. (17) in the form of Eq. (25).

$$\lambda_{1,2}^A = v_l \underbrace{\left[\frac{\alpha C_0 \left(\frac{\rho_g}{\rho_l} \right) \left(\frac{v_g}{v_l} \right) + 1}{\frac{\alpha C_0}{(1 - C_0 \alpha)} \left(\frac{\rho_g}{\rho_l} \right) + 1} \right]}_u \pm \underbrace{\sqrt{\frac{p}{\rho_l}} \cdot \sqrt{\frac{1}{1 - C_0 \alpha \left(1 - \frac{\rho_g}{\rho_l} \right)} + C_0 \left(\frac{\alpha (v_g - v_l) / c_g}{1 - C_0 \alpha \left(1 - \frac{\rho_g}{\rho_l} \right)} \right)^2}}_c \quad (25)$$

The first and second terms on the RHS of Eq. (25) are represented by u and c . For applications on gas-liquid flows in pipelines $u \ll c$, therefore the c term rules the behavior of the $\lambda_{1,2}$ eigenvalues families. An inspection on Eq. (25) reveals that $\lambda_{1,2} \sim \sqrt{p}$ and is supported by the exact values shown in Figure 2. For a given constant α , the ratio of eigenvalues laying on different pressure curves are proportional to the square root of the pressure ratio, for example: $\lambda_1^{100} / \lambda_1^{10} \cong \lambda_1^{10} / \lambda_1^1 \cong \sqrt{10}$. The dependence of $\lambda_{1,2}$ on α in c discloses that for $\alpha \rightarrow 0$ the eigenvalue grows unbounded, certainly this term is responsible for the large relative errors found when $\alpha \rightarrow 0$. The other extreme occurs for $\alpha \rightarrow 1$; the eigenvalues present a mild growth rate as α grows because the term within the 2nd square root of c grows as α approaches the unity. The same does not occurs with Gavage (1991) approximated eigenvalue because expressions lacks these correction terms.

22nd International Congress of Mechanical Engineering (COBEM 2013)
November 3-7, 2013, Ribeirão Preto, SP, Brazil

4. CONCLUSIONS

The approximated Jacobian matrix is hyperbolic and has real and distinct eigenvalues within 1% to the exact eigenvalues for $0.3 < \alpha < 0.99$. For $\alpha < 0.3$ the relative errors increase with the pressure, nonetheless for operational pressures of 1bar and 10bar the relative errors are bounded to 3%.

The simplification $(c_g/c_l)^2 \ll 1$ reduced the algebraic complexity of the Jacobian matrix allowing to express the eigenvalues through analytical expressions. The authors believe that this simplification will aid the deployment of linearization techniques to solve the system reducing the computational cost.

5. ACKNOWLEDGEMENTS

The authors would like thanks to Dr. Eduardo Gaspari for the fruitful discussions on the hyperbolicity matters. The authors acknowledge the financial support from Petrobras under contract number 0050-0075324.12.2

6. REFERENCES

- Bendiksen, K.H., 1984. "An experimental investigation of the motion of long bubbles in inclined tubes". *International Journal of Multiphase flow*, Vol. 10, No. 4, p. 467-483.
- Fjelde, K.K. and Karlsen, K.H., 2000. "A comparative study of some fully numerical shock-capturing schemes for simulating two-phase flow". April 5, 2000 <http://folk.uio.no/kennethk/articles/RF_report.pdf>.
- Flatten, T. and Munkejord, S.T., 2006. "The approximate riemann solver of roe applied to a drift-flux two-phase flow model ". *ESAIM: Mathematical Modelling and Numerical Analysis*, Vol. 4, No. 4, p. 735-764.
- Gavage, S.B., 1991. *Analyse numérique des modèles hydrodynamiques d'écoulements diphasiques stationnaires dans les réseaux de production pétrolière*. Ph.D. thesis, ENS, Lyon.
- Hibiki, T. and Ishii, M., 2003. "Distribution parameter and drift velocity of drift-flux model in bubbly flow". *International Journal of Heat and Mass Transfer*, Vol. 45, p. 707-721.
- Ishii, M., Chawla, T.C. and Zuber, N., 1976. "Constitutive equation for vapor drift velocity in two-phase annular flow". *AIChE Journal*, Vol. 22, No. 2, p. 283-289.
- Taitel, Y., Barnea, D., and Dukler, A.E., 1980. "Modeling flow pattern transition for steady upward gas-liquid flow in vertical tubes". *AIChE J.*, Vol. 26, No. 3, p. 345-354.
- Théron, B., 1989. *Écoulements diphasique stationnaires en conduite horizontale*. Ph.D. thesis, INP, Toulouse.
- Zuber, N. and Findlay, J.A., 1965. "Average volumetric concentration in two-phase flow systems". *Journal of Heat Transfer*, Vol. 87, No. 4, p. 453-468.
- Whitam, G.B., 1974. *Linear and Nonlinear Waves*. John Wiley & Sons Inc., 1st edition.

7. RESPONSIBILITY NOTICE

The authors are the only responsible for the printed material included in this paper.